Selected Paper

Lowest Electronically Excited Triplet States of 1,2,4,5-Tetracyanobenzene and Tetracyanopyrazine by Matrix-Isolation Infrared Spectroscopy Combined with a Density-Functional-Theory Calculation

Nobuyuki Akai, Isamu Miura, Satoshi Kudoh, Kiyotaka Shigehara,† and Munetaka Nakata*

Graduate School of BASE (Bio-Applications and Systems Engineering),
Tokyo University of Agriculture and Technology, Naka-cho, Koganei, Tokyo 184-8588

†Faculty of Technology, Tokyo University of Agriculture and Technology, Naka-cho, Koganei, Tokyo 184-8588

Received April 21, 2003; E-mail: necom@cc.tuat.ac.jp

The infrared spectra of photoexcited transient species produced during UV irradiation from 1,2,4,5-tetracyanobenzene (TCNB) and tetracyanopyrazine (TCNP) in low-temperature argon matrices were measured with a Fourier-transform infrared (FTIR) spectrophotometer. The produced transient species were identified as the lowest electronically excited triplet states, T_1, by a comparison of the observed infrared spectra with the calculated spectral patterns obtained by the hybrid density-functional-theory (DFT) method. The vibrational wavenumbers of the asymmetric C≡N stretching modes in the T_1 states were found to be shifted to the low-wavenumber side by about 150 cm^{-1}, indicating that the bonds of the cyano groups, –C≡N, in the T_1 states are close to cumulative double bonds, C=C=N. This observation is supported by calculations of the optimized geometrical structures and the Mulliken spin density obtained by the DFT method.

These days, vibrational spectroscopies combined with quantum chemical calculations have been rapidly developed to determine accurate molecular structures in the ground, S_0, state. For example, several conformational analyses of complicated molecules have been performed by low-temperature rare-gas matrix-isolation infrared spectroscopy with the hybrid density-functional-theory (DFT) method.[1–3] Almost all of the observed vibrational spectra in the S_0 state are found to be consistent with the corresponding spectral patterns calculated by the method.

In contrast to the S_0 state, it is difficult to measure the vibrational spectra in the lowest electronically excited triplet, T_1, state by standard spectroscopic methods. Even though the vibrational bands for the T_1 state can be measured by time-resolved Raman and infrared spectroscopies,[4–8] their observed bands are too broad to be comparable with the corresponding values obtained by the DFT method. On the other hand, the low-temperature matrix-isolation method can provide sharp infrared absorption bands of the T_1 states[8–13] when the sensitivity of an infrared detector is sufficiently high. We recently reported on the matrix infrared spectra and the optimized geometries obtained by DFT calculations for 1,2- and 1,4-dicyanobenzenes (DCNB) in the T_1 states, which lead to the conclusion that the benzene rings of 1,2- and 1,4-DCNBs in the S_0 states change to nearly quinonoid rings in the T_1 states, like *ortho*- and *para*-benzoquinones, respectively.[13] This finding seems to be important to understand the intermolecular interaction in the formation of charge-transfer (CT) complexes, because cyano-substituted benzenes play the role of electron-acceptor molecules in the CT complexes.[14–25]

In the present work, we performed similar experiments for 1,2,4,5-tetracyanobenzene (TCNB) and tetracyanopyrazine (TCNP) shown in Fig. 1. TCNB is one of the best-known electron-acceptor molecules to form CT complexes. Several experimental and theoretical studies of its monomer and CT complexes have been reported.[16–25] For example, Yoshino et al. investigated the photoreaction mechanism of a CT complex of TCNB with toluene upon UV irradiation, leading to the conclusion that 1-benzyl-2,4,5-tricyanobenzene and HCN are produced via a radical ion pair, i.e., the TCNB radical anion and the toluene radical cation.[14,15] We investigated the T_1 state of TCNB produced during UV irradiation in the present work, where infrared absorption bands were measured by FTIR spectroscopy, and the optimized geometry and Mulliken spin density were obtained by the DFT method.

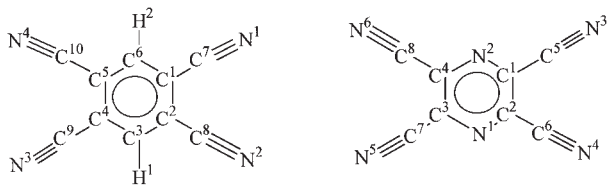

(a) 1,2,4,5-Tetracyanobenzene (TCNB) (b) Tetracyanopyrazine (TCNP)

Fig. 1. Numbering of atoms; (a) 1,2,4,5-tetracyanobenzene (TCNB) and (b) tetracyanopyrazine (TCNP).

In contrast to TCNB, fewer studies of TCNP have been reported. Despite that this molecule also shows electron affinity due to four cyano groups, and forms CT complexes with metal compounds, such as $Hg(O_2C_2F_3)_2$,[25] $Ru(NH_3)_5$,[26] and crown ether,[27] neither spectroscopic nor theoretical studies of

Published on the web October 15, 2003; DOI 10.1246/bcsj.76.1927

its monomer in the S_0 and T_1 states have been published, except for electron and chemical ionizations by mass spectrometry.[28,29] One of the purposes of the present work was to measure the infrared spectra of TCNP in the S_0 state, and to perform its accurate vibrational analysis with the aid of a DFT calculation. We also measured the infrared spectrum of TCNP in the T_1 state produced during UV irradiation, and compared it with that of TCNB and our previous results for 1,2- and 1,4-DCNBs.[13]

Experimental and Calculation Methods

A sample of TCNB was purchased from Tokyo Kasei Kogyo and used after twice re-crystallization from a methanol solution, while TCNP was synthesized by a condensation reaction between diiminosuccinonitrile and diaminomaleonitrile, following the literature.[30–32] A small amount of TCNB or TCNP was placed in a deposition nozzle with a heating system, on which argon gas (Nippon Sanso, 99.9999% purity) was flowed to achieve sufficient isolation of the sample. The samples of TCNB and TCNP were vaporized at 430 and 380 K, respectively. The mixed gas was deposited on a CsI plate, cooled by a closed-cycle helium refrigerator (CTI Cryogenics, Model M-22) to about 16 K. The infrared spectra of the matrix samples were measured with an FTIR spectrophotometer (JEOL, Model JIR-7000). The spectral resolution was 0.5 cm^{-1}, and the number of accumulation times was 64. Other experimental details were reported elsewhere.[8,12] UV radiation from a superhigh-pressure mercury lamp was used to increase the population of the T_1 states, where a water filter and a U330 bandpass filter ($200 < \lambda < 400$ nm) were used.

The DFT calculations were performed using the Gaussian 98 program.[33] The 6-31++G** basis set was chosen for TCNB, while the 6-31+G* basis set was used for TCNP, because the latter molecule includes no hydrogen atom. Becke's three-parameter hybrid density functional,[34] in combination with the Lee–Yang–Parr correlation functional (B3LYP),[35] was used to optimize the geometrical structure and to estimate the vibrational wavenumbers.

Results and Discussion

Infrared Spectra of 1,2,4,5-Tetracyanobenzene (TCNB). Before UV irradiation, we measured the matrix infrared spectrum of TCNB in the S_0 state to perform its vibrational analysis, because no accurate infrared spectrum had been reported. Figure 2 shows the observed spectrum of TCNB in a low-temperature argon matrix at 16 K along with the calculated spectral pattern obtained by the DFT/B3LYP/6-31++G** method, where a scaling factor of 0.98 is used. The calculated spectral pattern reproduces the observed spectrum satisfactorily, except for a few excess observed bands appearing at 1818, 1769 and 1245 cm^{-1} due to combination modes. The observed and calculated wavenumbers are summarized in Table 1 along with their infrared intensities. All of the bands for the infrared-active modes above 600 cm^{-1}, except for the much weaker b_{2u} mode, were observed and assigned. The calculated wavenumbers for the C–H and C≡N stretching modes are shifted from their observed values by about 100 and 50 cm^{-1}, respectively, because of vibration anharmonicity. The calculated values for the other modes are consistent with the corresponding observed values within about 10 cm^{-1}.

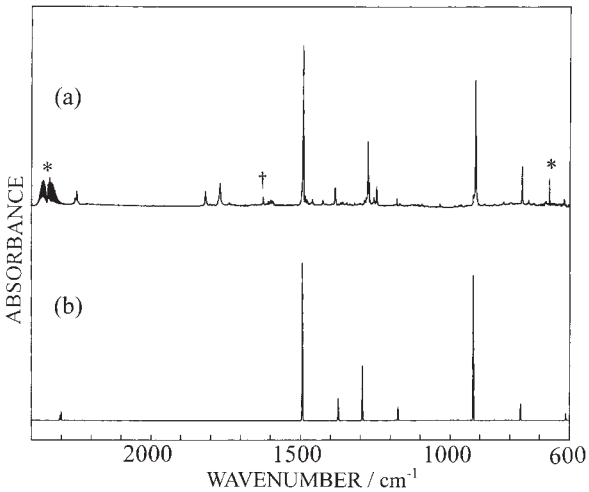

Fig. 2. Infrared spectra of 1,2,4,5-tetracyanobenzene; (a) observed spectrum in a low-temperature argon matrix at 16 K, where the bands marked with ∗ and † represent CO_2 in atmosphere and a small amount of water in the matrix, and (b) calculated spectral pattern obtained by the DFT/B3LYP/6-31++G** method, where a scaling factor of 0.98 is used.

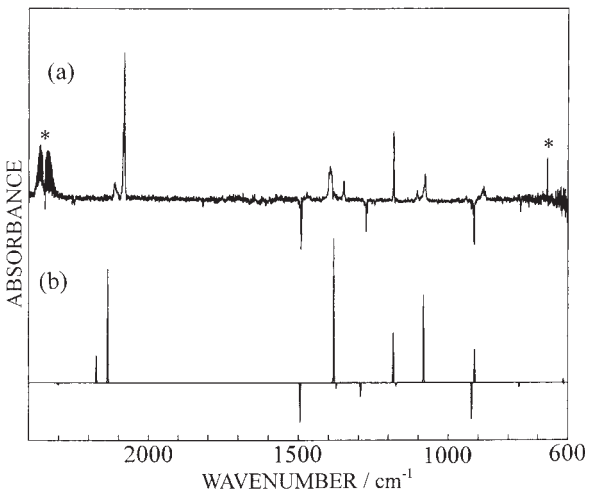

Fig. 3. Difference spectra of TCNB; (a) observed difference spectrum between those measured after and during UV irradiation and (b) calculated spectral pattern, where the T_1 and S_0 states are represented on the upside and downside, respectively.

Figure 3(a) shows a difference spectrum between those measured after and during UV irradiation through a U330 bandpass filter, where the increasing and decreasing bands are due to a photoinduced transient species and TCNB in the S_0 state, respectively. All of the transient bands disappeared after termination of the UV irradiation, and the original spectrum was completely reproduced, indicating that neither photodissociation nor photoisomerization of TCNB occurred upon this irradiation. The population of the transient species in the photo-steady state during UV irradiation was estimated to be about 1.5% from the decrease in the infrared band intensity for TCNB in the S_0 state. Since the lifetime of phospho-

Table 1. Observed and Calculated Wavenumbers (in cm^{-1}) of 1,2,4,5-Tetracyanobenzene in the S_0 and T_1 States

S_0 state					T_1 state					
Obs.		Calc.			Obs.		Calc.			
ν	Int.	ν[a)]	Int.[b)]	Sym.	ν	Int.	ν[a)]	Int.[b)]	Sym.	Assign.[c)]
		3169	0	a_g			3159	0	a_g	
3055	7.8	3168	15.7	b_{1u}			3158	5.1	b_{1u}	
2254	3.9	2305	2.9	b_{1u}			2205	0	a_g	
		2301	0	b_{3g}	2112	11.4	2174	19.2	b_{1u}	ν(C≡N)
2250	7.0	2301	5.7	b_{2u}	2081	100	2136	78.9	b_{2u}	ν(C≡N)
		2299	0	a_g			2134	0	b_{3g}	
1818	9.2									
1769	6.6									
		1606	0	b_{3g}			1395	0	a_g	
		1531	0	a_g			1390	0.2	b_{1u}	
1490	100	1494	100	b_{2u}	1394	25.2	1382	100	b_{2u}	β(C–H) + ν(ring)
					1348	16.7				comb.
1385	11.2	1374	13.8	b_{1u}			1344	0	b_{3g}	
1274	38.5	1293	34.5	b_{2u}			1339	0.0	b_{2u}	
		1265	0	b_{3g}			1281	0	a_g	
		1254	0	a_g	1182	49.5	1183	34.8	b_{1u}	β(ring)
1245	14.8				1102	8.0				comb.
		1183	0.1	b_{2u}	1077	18.2	1082	60.6	b_{2u}	ν(ring) + β(C–H)
1177	5.4	1174	8.5	b_{1u}			1067	0	b_{3g}	
		1044	0	b_{3g}			932	0	b_{3g}	
915	99.7	922	91.8	b_{3u}	882	10.1	912	23.1	b_{3u}	γ(C–H)
		916	0	b_{2g}			909	0	b_{2g}	
759	25.8	763	10.3	b_{2u}			738	0.0	b_{2u}	
		743	0	b_{2g}			661	0	b_{2g}	
		716	0	a_g			655	0	a_g	
		713	0	a_u			655	0	b_{3g}	
		680	0	b_{3g}			615	2.7	b_{1u}	
618	2.9	613	4.2	b_{1u}			612	0	a_u	

a) A scaling factor of 0.98 is used. b) Relative intensity in unit of km mol^{-1}. c) Symbols ν, β and γ represent stretching, in-plane bending and out-of-plane bending modes, respectively.

rescence in EPA glass at 77 K was reported to be 3.2 s,[36] we temporarily assigned the transient species to the T_1 state of TCNB produced by intersystem crossing from the S_n states. To confirm this assumption, we performed geometrical optimization and calculated the vibrational wavenumbers of the T_1 state by the DFT method. This calculation method can provide reliable infrared spectral patterns of the T_1 states as well as the S_0 states, as shown in our recent studies of naphthalene[8] and dicyanobenzenes.[13] Figure 3(b) shows a calculated spectral pattern for TCNB obtained by the DFT method, where the bands for the T_1 and S_0 states are displayed on the upside and downside, respectively. The calculated spectral pattern reproduces the observed spectrum satisfactorily. Thus, we conclude that the photoinduced transient species is assignable to the T_1 state of TCNB. The observed and calculated wavenumbers above 600 cm^{-1} are summarized in Table 1. The intensity of the band appearing at 1394 cm^{-1}, which shows broadening, is weaker than that of the corresponding calculated band,1382 cm^{-1}, probably because of the Fermi resonance with a combination band of 738 (b_{2u}) and 655 (a_g) cm^{-1}. The observed 1348 cm^{-1} band may be a counterpart of the Fermi resonance. The observed band appearing at 1102 cm^{-1} is assignable to a combination mode of the 655 (a_g) and 474 (b_{3u}) cm^{-1} bands.

Two intense bands of the transient species produced during UV irradiation, 2112 and 2081 cm^{-1}, are due to the asymmetric C≡N stretching modes, where their intensities are stronger than those of the corresponding bands in the S_0 state appearing at 2254 and 2250 cm^{-1}. The C–H out-of-plane bending mode appearing at 882 cm^{-1} in the transient state is shifted from that observed in the S_0 state, 915 cm^{-1}. Such large shifts for the C≡N stretching and C–H out-of-plane bending modes in the T_1 state to the low-wavenumber side were also found in 1,2- and 1,4-dicyanobenzenes.[13]

Infrared Spectra of Tetracyanopyrazine (TCNP). In contrast to TCNB, TCNP has not been investigated by any vibrational spectroscopies or theoretical methods, as described in Introduction. The matrix infrared spectrum measured before UV irradiation and the calculated spectral pattern of TCNP in the S_0 state obtained by the DFT method are shown in Fig. 4. The observed spectrum of TCNP is composed of only a few bands, because this molecule has no hydrogen atoms, but has a center of molecular symmetry. The calculated spectral pattern reproduces the observed spectrum as well as TCNB. The multiple bands around 1170 cm^{-1} may be ascribed to a combination of the 668 (a_g) and 484 (b_{1u}) cm^{-1} bands by Fermi resonance and/or a matrix-site effect.

After measuring the infrared spectrum of TCNP in the S_0

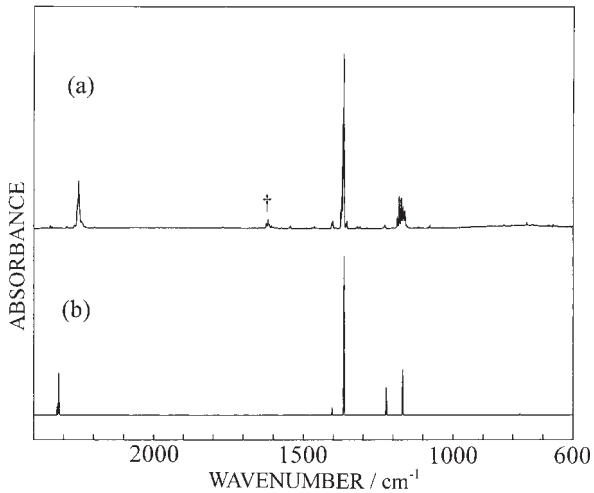

Fig. 4. Infrared spectra of tetracyanopyrazine; (a) observed spectrum in a low-temperature argon matrix at 16 K, where the bands marked with † represents a small amount of water in the matrix and (b) calculated spectral pattern obtained by the DFT/B3LYP/6-31+G* method, where a scaling factor of 0.98 is used.

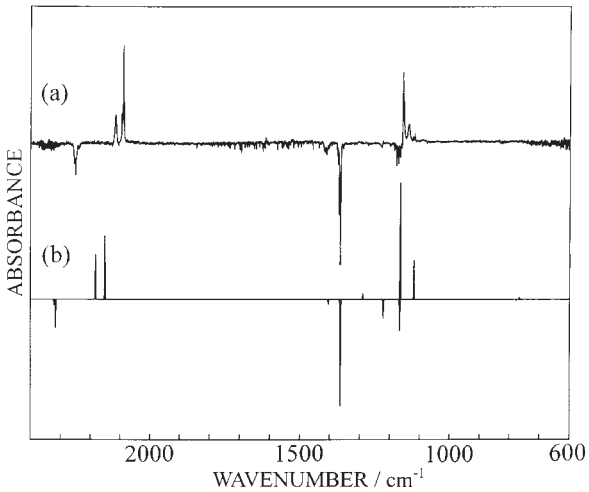

Fig. 5. Difference spectra of TCNP; (a) observed difference spectrum between those measured after and during UV irradiation and (b) calculated spectral pattern, where the T_1 and S_0 states are represented on the upside and downside, respectively.

state, we tried to measure the infrared spectrum of a photoexcited transient species. Figure 5 shows the difference spectrum between those measured after and during UV irradiation through a U330 bandpass filter. The decreasing and increasing bands are due to the S_0 state for TCNP and a photoinduced transient species, respectively. The calculated spectral pattern of the T_1 state is shown on the upside, while that of the S_0 state is on the downside. The calculated spectral pattern is consistent with the observed spectrum. We thus conclude that this transient species is assignable to the T_1 state of TCNP. The observed and calculated wavenumbers are summarized in Table 2 along with their intensities and vibrational mode symmetries. The observed intense bands appearing at 2115 and 2090 cm^{-1} are due to asymmetric C≡N stretching modes, while those appearing at 1157 and 1137 cm^{-1} are assignable to in-plane ring bending and stretching modes, respectively. Other infrared active modes are too weak to be detectable.

The bands of the C≡N stretching mode of TCNP in the T_1 state are shifted to the low-wavenumber side, like other cyano-substituted benzenes. It is noted that no band corresponding to the most intense band observed in the S_0 state, 1365 cm^{-1},

Table 2. Observed and Calculated Wavenumbers (in cm^{-1}) of Tetracyanopyrazine in the S_0 and T_1 states

S_0 state					T_1 state					
Obs.		Calc.			Obs.		Calc.			
ν	Int.	ν[a)]	Int.[b)]	Sym.	ν	Int.	ν[a)]	Int.[b)]	Sym.[c)]	Assign.[d)]
2254	16.3	2321	5.5	b_{1u}			2213	0	a_g	
		2317	0	b_{3g}	2115	28.0	2183	38.5	b_{1u}	ν(C≡N)
2250	25.7	2316	26.5	b_{2u}	2090	100	2151	54.3	b_{2u}	ν(C≡N)
		2314	0	a_g			2148	0	b_{3g}	
		1546	0	b_{3g}			1419	0.1	b_{1u}	
		1501	0	a_g			1352	0	a_g	
1402	3.9	1404	4.6	b_{1u}			1298	0	a_g	
1365[e)]	100	1364	100	b_{2u}			1290	4.8	b_{2u}	
		1281	0	a_g	1157	73.4	1165	100	b_{1u}	β(CNC)
1224[e)]	4.5	1222	17.5	b_{2u}	1137	21.3	1120	33.4	b_{2u}	ν(CNC)
1179[e)]	19.3	1167	28.7	b_{1u}			1078	0	b_{3g}	
		1083	0	b_{3g}			768	0	b_{3g}	
		804	0	b_{2g}			765	1.4	b_{2u}	
		776	0.7	b_{2u}			704	0	b_{2g}	
		729	0	a_u			629	0	b_{3g}	
		706	0	b_{3g}			617	0	a_g	
		688	0	a_g			605	0.1	b_{1u}	

a) A scaling factor of 0.98 is used. b) Relative intensity in unit of km mol^{-1}. c) The molecular structure in the T_1 state is assumed to D_{2h} symmetry. See text. d) Symbols ν and β represent stretching and in-plane bending modes, respectively. e) Bands exhibiting splitting.

which is assigned to the aromatic-ring stretching mode or C=C stretching mode, is observed in the T_1 spectrum. This implies that the aromatic character of the pyrazine ring in the S_0 state diminishes in the T_1 state. This speculation can be confirmed by the optimized geometry of TCNP, as described in the following section.

Geometrical Structures. The geometrical structure of TCNB in the S_0 state was previously investigated by gas-phase electron diffraction and theoretical calculations at the Hartree–Fock, Møller–Plesset second perturbation (MP2) and DFT/B3LYP levels. The determined experimental parameters were reproduced by the MP2 and DFT/B3LYP.[37] To compare the molecular structures of the S_0 states with those of the T_1 states, we recalculated the geometrical parameters of TCNB by the DFT method. On the other hand, no experimental values for the molecular structure of TCNP have been reported. The calculated values obtained in the present work are summarized in Tables 3 and 4 for TCNB and TCNP, respectively. The result of our calculation for TCNB in the S_0 state is consistent with that in a previous report.[37]

We also performed geometrical optimization for the T_1 states of TCNB and TCNP by the same method. The molecular structure of TCNB in the T_1 state belongs to the D_{2h} symmetry, like the S_0 state. The benzene ring is nearly regular hexagonal in the S_0 state, but distorted in the T_1 state; the C^1–C^2 bond in the S_0 state, 1.417 Å, lengthens to 1.513 Å in the T_1 state, while the C^2–C^3 bond is almost unchanged. On the other hand, the C≡N and C^1–C^7 lengths in the T_1 state are longer and shorter than the corresponding values in the S_0 state, respectively. This result suggests that the C–C≡N bond in the T_1 state is close to the cumulative double bonds, C=C=N, similarly to 1,2- and 1,4-dicyanobenzenes.[13]

Our DFT calculation on TCNP in the T_1 state shows that the optimized molecular geometry belongs to D_2 symmetry, where the cyano groups are slightly bent out of the pyrazine plane; the dihedral angle between the cyano group and the pyrazine ring is about 1°. Since the D_{2h} planar structure in the T_1 state has an imaginary wavenumber of -3 cm^{-1}, this structure is on a transition state. The single-point energy of the transition state is less stable than that of the D_2 structure by only 0.01 kJ mol^{-1}. Two schematic potential surfaces for the out-of-plane bending mode of the cyano groups of TCNB and TCNP are shown in Fig. 6.

The bond lengths of C^1–C^5, 1.437 Å, and C^5–N^3, 1.162 Å, for TCNP in the S_0 state change to 1.410 and 1.170 Å in the T_1 state, respectively, implying that the C–C≡N bonds in the T_1 state are close to the C=C=N bonds, like the cyano-substitut-

Table 3. Geometrical Parameters of 1,2,4,5-Tetracyanobenzene in the S_0 and T_1 States

Parameter[a)]	S_0 state		T_1 state
	Obs.[b)]	Calc.[c)]	Calc.[c)]
	Bond length (in Å)		
C^1–C^2	1.413 (6)	1.417	1.513
C^2–C^3	1.403 (4)	1.399	1.395
C^1–C^7	1.429 (3)	1.433	1.406
C–H	1.050 (16)	1.084	1.085
C–N	1.161 (2)	1.163	1.171
	Bond angle (in deg.)		
C^1–C^2–C^3	121.0 (2)	119.7	119.2
C^2–C^3–C^4	118.0 (4)	120.6	121.6
C^2–C^1–C^7	120.8 (3)	121.1	120.2
C^1–C^7–N^1		178.7	180.0

a) Numbering of atoms is defined in Fig. 1. b) Electron diffraction data in the gas phase.[37] c) Obtained by the DFT/B3LYP/6-31++G** method.

Table 4. Calculated Geometrical Parameters of Tetracyanopyrazine in the S_0 and T_1 States Obtained by the DFT/B3LYP/6-31+G* Method

Parameter[a)]	S_0 state	T_1 state
	Bond length (in Å)	
C^1–C^2	1.419	1.523
C^1–C^5	1.437	1.410
C^1–N^2	1.335	1.329
C^5–N^3	1.162	1.170
	Bond angle (in deg.)	
C^1–C^2–N^1	121.3	120.7
C^2–N^1–C^3	117.4	118.5
C^2–C^1–C^5	121.2	120.3
C^1–C^5–N^3	179.1	178.2

a) Numbering of atoms is defined in Fig. 1.

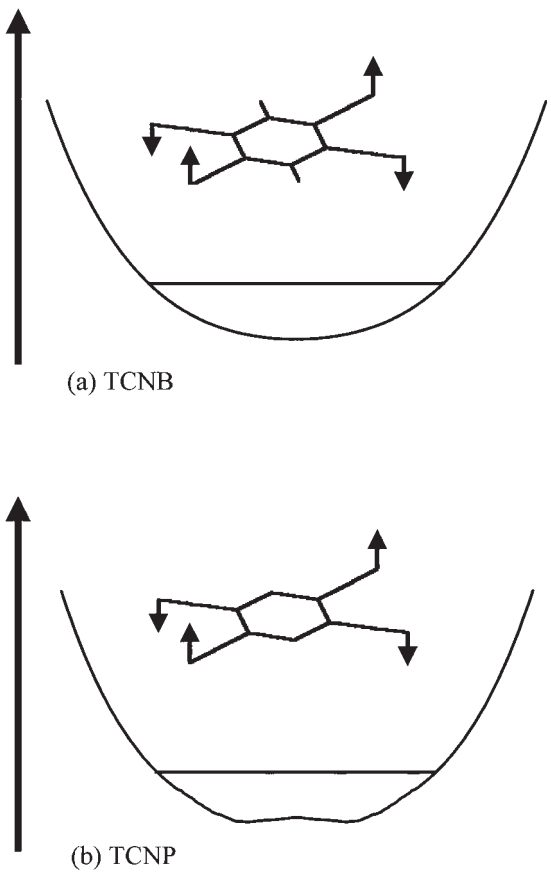

Fig. 6. Schematic potential surfaces of cyano-group out-of-plane bending modes for (a) TCNB and (b) TCNP in the T_1 states.

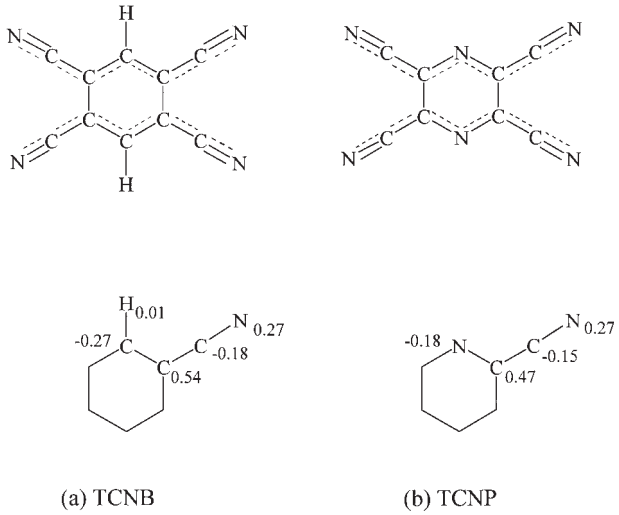

Fig. 7. Schematic molecular structures and the Mulliken spin densities for (a) TCNB and (b) TCNP in the T_1 states.

ed benzenes. The pyrazine ring is also distorted like the benzene ring of TCNB; the C^1–C^2 length in the T_1 state is longer than that in the S_0 state by about 0.1 Å, while the C^1–N^2 length is unchanged within 0.01 Å. These findings suggest that the bond order of C^1–C^2 in the S_0 states, 1.5, decreases to 1 in the T_1 states, while those of C^1–C^6 for TCNB and C^1–N^2 for TCNP remain unchanged. Thus, the π-electron conjugated systems of TCNB and TCNP are separated into two parts, NCCCCCN and NCCNCCN, respectively. The schematic bond orders of TCNB and TCNP in the T_1 states are shown in Fig. 7. We thus conclude that the infrared bands of the asymmetric C≡N stretching mode in the T_1 state show a large shift to the low-wavenumber side caused by the structural change from C–C≡N to C=C=N. This is supposed by the Mulliken spin density distributions calculated by the DFT method. Figure 7 shows the result of a calculation that unpaired electrons are located on the C^1 and N^1 atoms for TCNB and C^1 and N^3 atoms for TCNP. The localization of spin can be explained by six possible resonance contributions, shown in Fig. 8, when the structural change from C–C≡N to C=C=N is considered.

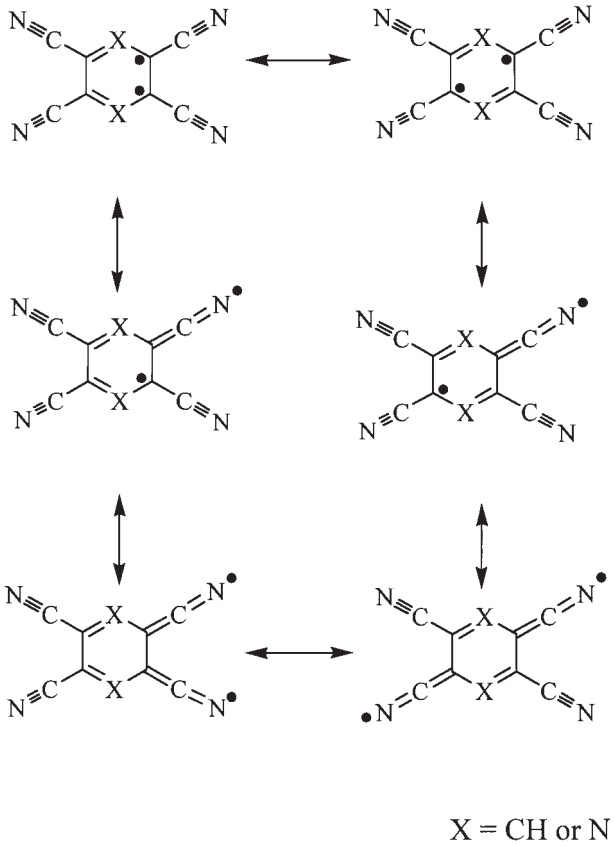

Fig. 8. Six possible resonance contributions for TCNB and TCNP.

Comparison of TCNB, TCNP and DCNBs in the T_1 states. The differences between the S_0 and T_1 states for TCNB, TCNP and DCNBs obtained in the present work are summarized in Table 5. It is noted that (1) the wavenumber shifts of the C≡N stretching and C–H out-of-plane bending modes for DCNBs are larger than those of TCNB and TCNP; (2) the changes in the C≡N and C–C lengths in the C–C≡N group for DCNBs are lager than those for TCNB and TCNP; (3) the Mulliken spin densities on the terminal atoms in the C–C≡N group for DCNBs are lager than those of TCNB and TCNP. These results suggest that the C–C≡N groups in

Table 5. Comparison of Differences between the S_0 and T_1 States and Spin Densities for DCNBs, TCNB and TCNP

	1,2-DCNB[a)]	1,4-DCNB[a)]	TCNB	TCNP
Mode[b)]		Wavenumbers shifts (in cm^{-1}) from S_0 to T_1		
ν(C≡N)	−172	−251	−169/−142	−160/−139
γ(C–H)	−111	−93	−33	
Bond[c)]		Bond length changes (in Å) from S_0 to T_1		
C≡N	0.015	0.016	0.008	0.008
C–C	−0.043	−0.047	−0.027	−0.027
		Mulliken spin density[d)]		
C–C–N	0.65	0.70	0.54	0.47
C–C–N	−0.21	−0.23	−0.18	−0.15
C–C–N	0.36	0.40	0.27	0.27

a) From Ref. 13. b) Symbols ν and γ represent stretching and out-of-plane bending modes. c) C≡N and C–C parts in C–C≡N bond. d) Mulliken spin density on atom underlined.

the T_1 states for DCNBs are closer to the cumulative double bonds, C=C=N, than those for TCNB and TCNP. This may be ascribed to the size of the π-electron conjugated system; the π-electron conjugated systems for TCNB and TCNP are separated into the two parts of NCCCCCN and NCCNCCN, respectively, while those for DCNBs spread overall on the molecules. However, further experimental and theoretical information is necessary to confirm this speculation.

The authors thank Professors Kozo Kuchitsu and Masao Takayanagi (BASE, Tokyo University A & T) for their helpful discussions.

References

1 S. Kudoh, M. Takayanagi, M. Nakata, T. Ishibashi, and M. Tasumi, *J. Mol. Struct.*, **479**, 41 (1999).
2 N. Nagashima, S. Kudoh, M. Takayanagi, and M. Nakata, *J. Phys. Chem. A*, **105**, 10832 (2001).
3 N. Akai, S. Kudoh, M. Takayanagi, and M. Nakata, *J. Phys. Chem. A*, **106**, 11029 (2002).
4 G. Balakrishman and S. Umapathy, *J. Chem. Soc., Faraday Trans.*, **93**, 4125 (1997).
5 Y. Uesugi, M. Mizuno, A. Shimojima, and H. Takahashi, *J. Phys. Chem. A*, **101**, 268 (1997).
6 M. Puranik, J. Chandrasekhar, and S. Umapathy, *Chem. Phys. Lett.*, **337**, 224 (2001).
7 D. Pan, L. C. T. Shoute, and D. L. Phillips, *J. Raman Spectrosc.*, **31**, 255 (2000).
8 M. Nakata, S. Kudoh, M. Takayanagi, T. Ishibashi, and C. Kato, *J. Phys. Chem. A*, **104**, 11304 (2000).
9 M. B. Mitchell, G. R. Smith, and W. A. Guillory, *J. Chem. Phys.*, **75**, 44 (1981).
10 J. Baiardo, R. Mukherjee, and M. Vala, *J. Mol. Struct.*, **80**, 109 (1982).
11 H. Krumschmidt and C. Kryschi, *Chem. Phys.*, **154**, 459 (1991).
12 S. Kudoh, M. Takayanagi, and M. Nakata, *J. Mol. Struct.*, **475**, 253 (1999).
13 N. Akai, S. Kudoh, and M. Nakata, *Chem. Phys. Lett.*, **371**, 655 (2003).
14 A. Yoshino, M. Ohashi, and T. Yonezawa, *J. Chem. Soc., Chem. Commun.*, **1971**, 97.
15 A. Yoshino, K. Yamasaki, T. Yonezawa, and M. Ohashi, *J. Chem. Soc., Perkin Trans. 1*, **1975**, 735.
16 J. Prochorow, *J. Mol. Struct.*, **404**, 199 (1997).
17 J. Prochorow and I. Deperasińska, *J. Mol. Struct.*, **450**, 47 (1998).
18 B. T. Lim, S. Okajima, A. K. Chandra, and E. C. Lim, *J. Chem. Phys.*, **77**, 3902 (1982).
19 B. R. Arnold, A. W. Schill, and P. V. Poliakov, *J. Phys. Chem. A*, **105**, 537 (2001).
20 S. Aich and S. Basu, *Chem. Phys. Lett.*, **281**, 247 (1997).
21 S. Ghosh, C. Stuart, A. Ozarowski, A. Misra, and A. Maki, *Chem. Phys. Lett.*, **368**, 495 (2003).
22 S. Iwata, J. Tanaka, and S. Nagakura, *J. Am. Chem. Soc.*, **89**, 2813 (1967).
23 H. Hayashi, S. Nagakura, and S. Iwata, *Mol. Phys.*, **13**, 489 (1967).
24 H. Hayashi, S. Iwata, and S. Nagakura, *J. Chem. Phys.*, **50**, 993 (1969).
25 S. Fukuzumi and J. K. Kochi, *J. Org. Chem.*, **46**, 4116 (1981).
26 M. Moscheroch, E. Waldhoer, H. Binder, W. Kaim, and J. Fiedler, *Inorg. Chem.*, **34**, 4326 (1995).
27 R. Malin, *Bull. Soc. Chim. Belg.*, **89**, 359 (1980).
28 C. N. McEwen and M. A. Rudat, *J. Am. Chem. Soc.*, **103**, 4343 (1981).
29 G. Holzmann and H. W. Rothkopf, *Org. Mass Spectrom.*, **13**, 636 (1978).
30 W. A. Sheppard, R. W. Begland, A. Cairncross, D. S. Donald, D. R. Hartter, and O. W. Webster, *J. Am. Chem. Soc.*, **93**, 4953 (1971).
31 R. W. Begland, D. R. Hartter, D. S. Donald, A. Cairncross, and W. A. Sheppard, *J. Org. Chem.*, **39**, 1235 (1974).
32 R. W. Begland, D. R. Hartter, F. N. Jones, D. J. Sam, W. A. Sheppard, O. W. Webster, and F. J. Weigert, *J. Org. Chem.*, **39**, 2341 (1974).
33 "GAUSSIAN 98" was employed for the calculations. M. J. Frisch, G. W. Trucks, H. B. Schlegel, G. E. Scuseria, M. A. Robb, J. R. Cheeseman, V. G. Zakrzewski, J. A. Montgomery, R. E. Stratmann, J. C. Burant, S. Dapprich, J. M. Millam, A. D. Daniels, K. N. Kudin, M. C. Strain, O. Farkas, J. Tomasi, V. Barone, M. Cossi, R. Cammi, B. Mennucci, C. Pomelli, C. Adamo, S. Clifford, J. Ochterski, G. A. Peterson, P. Y. Ayala, Q. Cui, K. Morokuma, D. K. Malick, A. D. Rabuck, K. Raghavachari, J. B. Foresman, J. Cioslowski, J. V. Ortiz, B. B. Stefanov, G. Liu, A. Liashenko, P. Piskorz, I. Komaromi, R. Gomperts, R. L. Martin, D. J. Fox, T. Keith, M. A. Al-Laham, C. Y. Peng, A. Nanayakkara, C. Gonzalez, M. Challacombe, P. M. W. Gill, B. G. Johnson, W. Chen, M. W. Wang, J. L. Andres, M. Head-Gordon, E. S. Replogle, and J. A. Pople, Gaussian, Inc., Pittsburgh PA (1998).
34 A. D. Becke, *J. Chem. Phys.*, **98**, 5648 (1993).
35 C. Lee, W. Yang, and R. G. Parr, *Phys. Rev. B: Condens. Matter*, **37**, 785 (1988).
36 Y. Achiba and K. Kimura, *Chem. Phys. Lett.*, **48**, 107 (1977).
37 G. Schultz, Á. Szabados, G. Tarczay, and K. Zauer, *Struct. Chem.*, **10**, 149 (1999).